sustainability

MDPI

Article

Meteorological Effects of Green Infrastructure on a Developing Medium Latin American City: A Numerical Modeling Assessment

Otavio Medeiros Sobrinho [1,2,*], Anderson Paulo Rudke [1,2], Marcos Vinicius Bueno de Morais [3] and Leila Droprinchinski Martins [1]

[1] Graduate Program in Environmental Engineering, Campus Londrina, Federal University of Technology, Paraná, Av. dos Pioneiros, 3131, Londrina 86036-370, Brazil
[2] Graduate Program in Sanitation, Environment and Water Resources, School of Engineering, Federal University of Minas Gerais, Av. Presidente Antônio Carlos, 6627, Belo Horizonte 31270-901, Brazil
[3] Departamento de Obras Civiles, Facultad de Ciencias de la Ingeniería, Universidad Católica del Maule, Av. San Miguel, 3605, Talca 346000, Chile
* Correspondence: sobrinhotavio@gmail.com

Abstract: Urban areas concentrate more than 50% of the world's population and are highly impacted by human activities, mainly due to high population density, directly affecting the micro-climate. In this sense, green infrastructures (GIs) have been pointed out to be helpful in mitigating these effects in large urban areas, where most of the studies were conducted. Therefore, this study evaluates the impacts on meteorological variables in a medium-sized city through the Weather Research and Forecasting model by implementing urban classes of Local Climate Zones (LCZ). Five urban parks and an urban lake were identified and expanded in the inner model grid to analyze the effects of GIs on meteorological variables in the urban environment. Results show that the 10 m wind speed can present an improvement for all statistical indices due to the better vertical representation of urban structures in the central urban area by the LCZ urban classes. In addition, green areas contributed locally to reducing the urban heat island (UHI) effects, resulting in cooling rates around these infrastructures. Compared to the lake, the use of the urban LCZ classes has proven to be an effective way to improve the representation of meteorological variables by a mesoscale weather model. Regarding GIs, this practice performs environmental services capable of mitigating the effects of UHI, sustaining the importance of these systems in urban projects, even for medium-sized cities. Finally, these findings provide support for public decision-makers in creating Master Plans for medium-sized cities regarding the implementation of GIs.

Keywords: urban parks; urban planning; sustainable cities; thermal mitigation strategies

Citation: Sobrinho, O.M.; Rudke, A.P.; Morais, M.V.B.d.; Martins, L.D. Meteorological Effects of Green Infrastructure on a Developing Medium Latin American City: A Numerical Modeling Assessment. *Sustainability* **2023**, *15*, 1429. https://doi.org/10.3390/su15021429

Academic Editors: Natale Arcuri, Piero Bevilacqua, Antonio Gagliano and Stefano Cascone

Received: 14 November 2022
Revised: 31 December 2022
Accepted: 6 January 2023
Published: 11 January 2023

1. Introduction

Population growth enhanced from industrial revolutions is the main cause of the urban expansion in progress, increasing the consumption of natural resources. Consequently, it has been causing large-scale effects worldwide, such as climate change and its consequences [1–4]. Natural areas covered by croplands, vegetation, and/or pasturelands have been converted to build surfaces through the urbanization process that reduce the albedo [5,6]. This radiation absorbed during the day is dissipated by sensitive heat, enhancing the urban heat island (UHI) [7–10].

The need for air-conditioning systems in indoor places grows when temperatures rise over central urban centers as a result of urbanization and climate change, directly causing higher energy consumption and influencing the outdoor environment [11]. One solution that can lead to thermal comfort in indoor–outdoor environments is green infrastructures (GIs), which contribute to mitigating the effect of UHI, besides reducing energy

consumption for cooling buildings in the summertime [12–16]. GIs are defined as urban areas covered by vegetation of any size, in private and public spaces, regardless of size and function, and may include small water bodies such as ponds, lakes, or streams [17,18]. The vegetation in urban areas modifies the surface energy budget, increasing the latent heat flux and reducing outdoor temperature [19,20]. For example, in rooftop gardens on multi-store car parks, the inclusion of GIs in Singapore reduced the near-surface air temperature by about 1 to 2 °C during the nighttime in the western part of the city [21].

Nevertheless, there are also limitations to the GIs [22–24]. For example, in Porto's urban area, the influence of a set of resilience measures on the wind flow and air pollutant dispersion was evaluated [22]. Overall, they observed that the implementation of GIs improved air quality, mainly due to enhanced ventilation and dispersion capacity. Furthermore, according to the GI characteristic, urban geometry can influence air quality, with high vegetation canopies in urban canyons resulting in lower air quality since taller trees cause canyon flow change [25]. In fact, low vegetation is more appropriate in canyon areas as it improves local air quality [26].

GI has been shown to have many benefits for urban areas, including mitigating the impacts of urbanization on the environment and improving quality of life for residents. However, as mentioned, there are also limitations to consider when implementing GI [27]. Moreover, regarding choosing the adequate GI for the region, another relevant aspect is the maintenance and cost associated with it. For example, the cost of implementing a living wall ranged from EUR 2000 to 3000 in 2020, and the charge of maintaining urban parks, including planting, pruning, pest and disease management, and removal, can also vary greatly depending on the species chosen, reaching no more than USD seven per tree species per year [28,29]. It is therefore important for cities to carefully consider the benefits and limitations of GI in light of their specific urban characteristics and climate [30,31].

Not only are the urbanization effects restricted to large metropolitan regions, but they are also reported in smaller cities [32–34]. According to the World Urbanization Prospects, 55% of the world population resides in urban areas, where 5.4% live in cities between 500,000 and 1 million inhabitants [33]. In addition, recent projections for 2050 show that 68% of the world's population will reside in urban areas, increasing the population density in metropolitan centers [35]. The higher growth rates are observed in town centers with less than 500,000 inhabitants [35,36]. Few studies have evaluated the urbanization effects and green strategies on meteorological variables through numerical models in medium-sized cities in Latin American countries such as Brazil [6,37–39].

Therefore, numerical modeling can be used to reduce the costs of evaluating the implementation of GIs, even considering their limitations [20]. In a study conducted in Tehran, Iran, the impact of GI implementation on the UHI effect was examined using a combination of the WRF model and the Single Layer Urban Canopy Model. The results demonstrated that introducing green spaces led to a 25% reduction in the daytime Turbulence Kinetic Energy budget and a decrease of 0.2 K in the potential temperature [40]. Additionally, Li et al. [41] used WRF in conjunction with the Princeton Urban Canopy Model to investigate the UHI during a heat wave. They found that an increase in GI would result in a nearly linear reduction of the surface and near-surface UHIs.

Hence, more investigations by numerical models should be performed for emerging metropolitan areas, which are growing fast and request more sustainable urban planning. These simulations require a better description of the local characteristics of the urban area [42,43], in which Local Climate Zones (LCZs) have been provided to improve representation [44,45]. Therefore, this paper focuses on the numerical analysis of the role of GI (park and lake) areas in the urban atmosphere of a medium-sized city while using the LCZ to improve urban representation.

2. Methods

2.1. Study Area

The region of this study comprises the Metropolitan Area of Londrina (MAL), located in the state of Paraná, Southern Brazil, which has a population characteristic of medium urbanizations, between 1 and 5 million inhabitants (Figure 1). The MAL consists of 25 cities, in 7440 km^2, where approximately 50% of the population live in Londrina (about 575,000 inhabitants) [36]. Londrina has a humid subtropical climate, Cfa classification, with average temperatures above 22 °C in the summer and accumulated monthly rainfall above 60 mm in the winter [46,47].

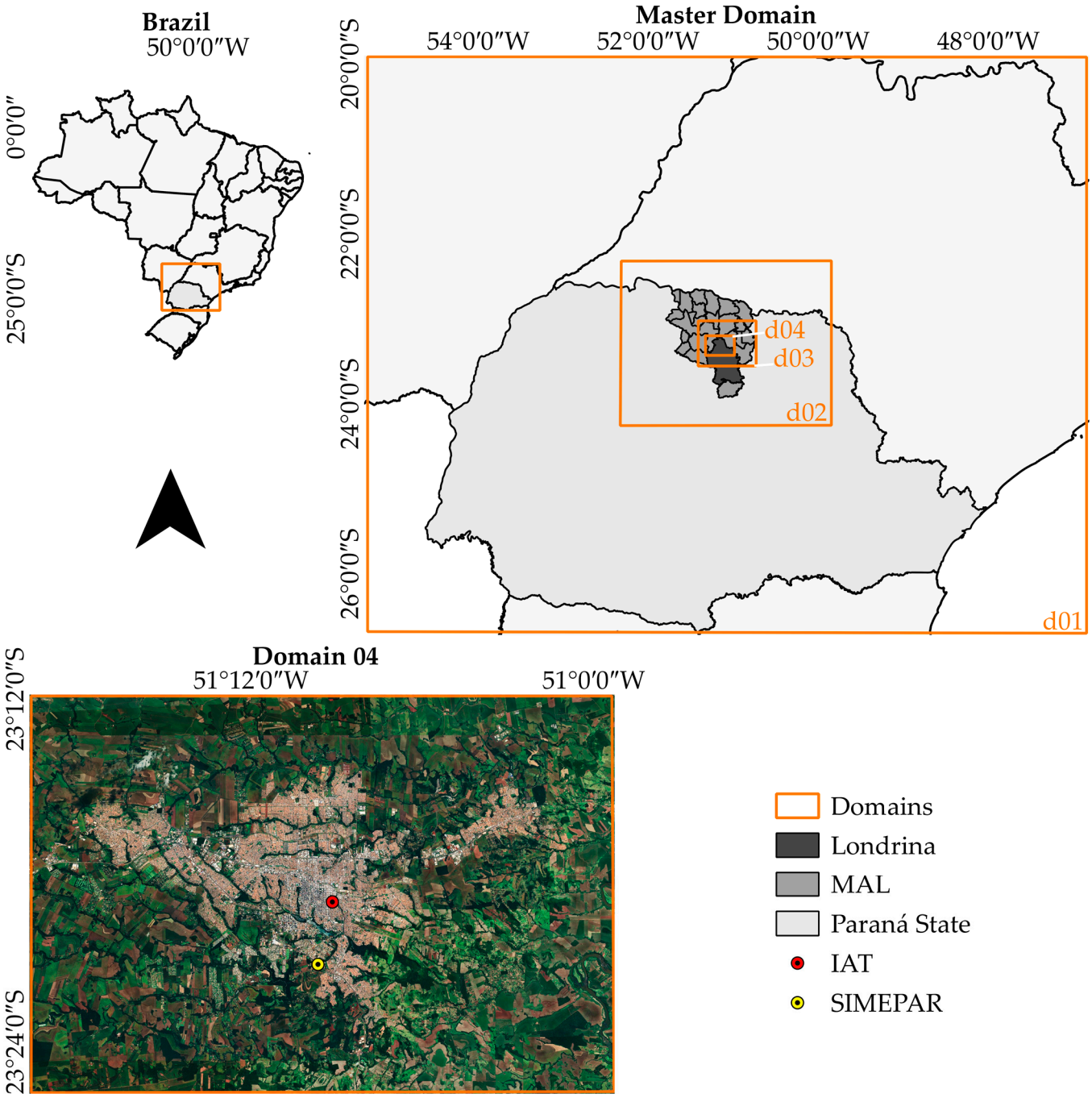

Figure 1. Location and simulation domains of the study area. Red and yellow points are, respectively, the location of stations from Instituto Água e Terra (IAT) and Sistema Meteorológico do Paraná (SIMEPAR).

2.2. Modeling System

The simulations were carried out with the Weather Research and Forecast model (WRF) version 4.1.5, originally developed by the National Center for Atmospheric Research (NCAR). It is a multi-scale, non-hydrostatic tool. The Eulerian model was used, with fixed space, and applied to atmospheric research and operational forecasting [48,49].

Three nested domains were constructed, centralized at 23.30° S and 51.10° W with 9, 3, and 1 km of the horizontal spacing grid, and a fourth internal domain at 23.31° S and 51.16° W (0.333 km of grid point spacing), covering the urban area of Londrina, were used for the simulations (Figure 1 and Table 1).

Table 1. Configuration of simulation domains.

Domain	Grid Points Spacing (km)	Grid Points		Domain Size (km^2)	Vertical Levels
		X	Y		
d01	9	100	80	900 × 720	33
d02	3	88	70	264 × 210	33
d03	1	76	58	76 × 58	33
d04	0.333	106	79	34.3 × 26.3	33

The physical and surface parameterization used in this study, shown in Table 2, were validated in previous studies in Brazil for the region [19,42,50–54]. Therefore, they were used in this study area. The output of the Global Data Assimilation System/Final (GDAS/FNL, [55]) was used as atmospheric initial and boundary conditions. This dataset has a horizontal spacing grid of 0.25° and 26 vertical levels, a temporal resolution of 6 h, and top of the atmosphere of approximately 10 hPa.

Table 2. Physical parameterizations considered in the WRF model.

Physics Options	Scheme	Reference
Longwave Radiation Shortwave Radiation	New Goddard scheme	[56]
Surface Layer	Revised MM5	[57]
Land Surface	Noah	[58]
Boundary Layer	YSU	[59]
Microphysics	Pardue Lin	[60]
Urban Surface	BEP	[61]

Numerical simulations were executed from 2017, September 6th 00 UTC to September 16th 00 UTC (240 simulated hours), since it was a period of relatively calm winds, clear-sky days, and no rainfall. The first 24 h of simulation were discarded from the analysis to avoid the spin-up effect [62,63]. The model performance analysis was conducted evaluating the values obtained from the model with those measured at the IAT and SIMEPAR monitoring stations (Figure 1) by using Pearson's Correlation Coefficient (r), Mean Bias (MB), Root-Mean-Square Error (RMSE), and Pielke skill score (S_{Pielke}) [62,64,65]. The IAT station (latitude: 23.319° S; longitude: 51.155° W) is located in the central area of Londrina, set and funded by Instituto Água e Terra (Figure S1), while SIMEPAR (latitude: 23.355° S; longitude: 51.161° W) is in the south of surrounding areas of Londrina, supported by Sistema Meteorológico do Paraná and Instituto de Desenvolvimento Rural do Paraná (Figure S1). These are the meteorological stations with observations available in the simulation period in the study region used for validation.

LCZ data were developed regarding urban characteristics, enabling the input data improvement for using Building Environment Parameterization (BEP; [61]), trying to better represent the turbulent moment fluxes in urban areas [50,66]. An accurate data set and a proper urban land use parameterization are critical for the mesoscale model to represent UHI effects [67].

This study used the LCZ classification [68]. Level "0" provides comprehensive and consistent information on urban surface coverage using multi-spectral satellite images of Landsat 8 [69]. The representation of urban areas is due to the categorized classification, in which each LCZ class is associated with a range of spectral values for the main descriptors of the urban surface [70].

By using a supervised classification method, the classifier requires training samples that will be used to establish the spectral signatures of each class stipulated in the LCZ scheme. The LCZ classification for MAL followed the World Urban Database and Access Portal Tools (WUDAPT) guide (available at http://www.wudapt.org, accessed on 9 October 2020), from collecting training samples to supervised classification. Urban canopy parameters (fraction of the urban landscape that does not have natural vegetation; heat capacity, thermal conductivity, surface albedo, and surface emissivity of the roof, building wall and ground; roughness length for momentum over the ground, and roof; height and width of buildings; width and direction from the north of streets) were obtained from documents available with the LCZ preparation process on the WUDAPT website [68,71].

To assess whether LCZ reliably represents the terrestrial surface for middle-size urban areas, it is necessary to validate the mapping. The validation process seeks to statistically verify whether the entire surface is well represented by the land cover map [43]. In this study, accuracy was quantified only for the urban classes in Londrina, as it corresponds to the innermost domain area. The determination of the validation sample size was based on Congalton and Green [72], who suggest collecting 50 samples for each land cover class in mappings performed for areas smaller than 0.4 million hectares and a classification scheme with less than 12 classes. As in minority classes, classes with total pixels less than 50 (Open midrise and Lightweight low-rise), it is not possible to collect 50 samples; therefore, we adopted 50% of the total amount of pixels as validation samples. This process was adopted as an adjustment based on the relative importance of these classes and to prevent changes in the accuracy due to map classes with low representation in the study area (Open midrise and Lightweight low-rise classes together represent less than 1% of the study area) [72].

The BEP scheme allows the WRF model to represent the direct interaction of the buildings with the atmosphere (wind speed, potential temperature, and turbulent kinetic energy) through geometric, thermal, and aerodynamic properties of different urban land uses [61,73–75]. Each class of urban canopy is characterized by the homogenous grouping of urban structures considering the same width, separated at the same distance (canyon wide), and with different building heights (see characteristics of LCZ urban classes in Table S1) [61].

The urban classes of LCZ and BEP scheme were activated only for smaller domains (d03 and d04) due to model resolution, enabling the possibility to evaluate the effects of urbanization in greater detail and demand less computational time.

2.3. Experimental Configuration

Simulations were achieved using the schemes and configurations mentioned. Firstly, a preliminary analysis evaluated the use of LCZ by comparison of performance indexes (domain d03) in the simulations using the default land use obtained by Moderate-Resolution Imaging Spectroradiometer (MODIS) and implementing urban LCZ classes, namely DEFAULT and Simulation A (SA) simulations, respectively.

Subsequently, in the innermost domain, simulations were performed to obtain the meteorological impacts of GIs, considering the LCZ classes for urban areas. In this sense, an artificial lake built in 1959 in the city to solve the drainage problems hampered by a natural stone dam was considered. However, the MODIS land cover classification was not originally able to identify this lake in the city. Thus, we call Simulation B the same as SA, identifying the lake surface (class 17) to better represent the land use conditions of the study area.

In SC, the five urban parks that do not exist in the MAL were carefully thought of and located in SC to allow the evaluation of the green areas (parks) in the urban meteorological variables (see Table S2 for GI size and grid points). The locations of parks used in the simulations follow the Master Plan of Londrina (an urban planning with guidelines and rules for ordering the city territory, with definitions of occupation zones for residential, industrial and commercial purposes, etc.), which declares that urban parks can be implemented in regions with low population density and irregular occupation [76]. Furthermore, to define the location and size of the parks, we took into consideration the natural water bodies, remaining vegetation, and valleys existing in the urban area. A brief summary of the simulations is presented in Table 3.

Table 3. Summary of simulation features.

Simulation	Land Use
Evaluation of the implementing urban LCZ classes	
DEFAULT	MODIS (16 natural classes and an urban class)
SA	MODIS + LCZ (16 natural classes by MODIS and 10 urban classes by LCZ product)
Evaluation of the GIs	
SB	Same as SA but identifying the lake surface
SC	Same as SB with the inclusion of five urban parks

The categorization of GIs was based on the classification scheme proposed by the International Geosphere–Biosphere Program (IGBP), which is used in the MODIS land cover legend. Therefore, the lake was classified as a water body, represented by the number 17 in the IGBP scheme. The urban parks were categorized as evergreen broadleaf forest (class number 2 in IGBP) due to the phytophysiognomy of the native cover of the MAL.

3. Results and Discussion

The results presented in this section are for the innermost domains (d03 and d04) of the model, comparing the simulated results for DEFAULT and SA to infer LCZ application in the representation of surface data and comparing SA, SB, and SC simulations to study the effects of GIs. The data analyzed were, namely, temperature and specific humidity at 2 m (T2 and Q2), 10 m wind speed (WS10), and surface energy fluxes at local time (UTC-3).

3.1. Local Climate Zones

Figure 2a shows the LCZ urban classification for domain d04 and Figure 2b includes the identification of urban GIs (parks and lake). The validation results indicate that the LCZ urban classification has an overall accuracy of 67% (see Table S3 in the Supplementary Materials), which is considered consistent according to studies already carried out using LCZ [77]. The classification of LCZ could not determine urban areas with high and medium density (classes 31, 32, and 35, of Figure 2) due to the inhomogeneity of the characteristics of these classes for Londrina. In contrast, that classification showed high performance on the representation of classes 36, 37, and 39 (accuracy >80%). Both meteorological stations, IAT and SIMEPAR, are located in compact midrise areas (class 32 in Figure 2).

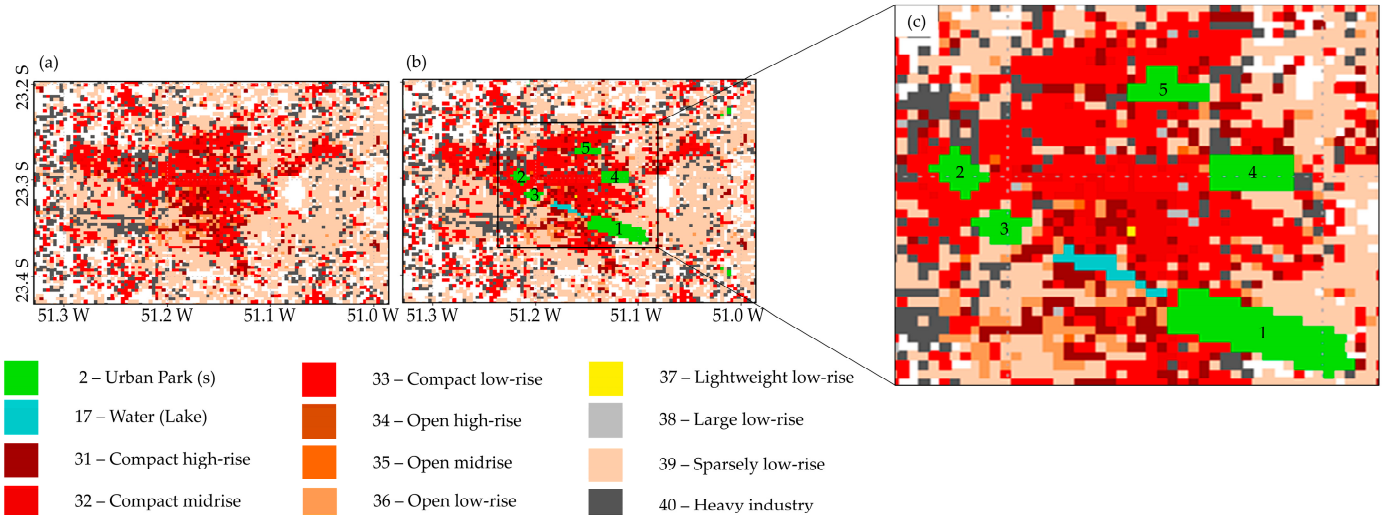

Figure 2. Local Climate Zone urban classification for MAL (d04), (**a**) WUDAPT level "0", (**b**) GIs (2—urban parks, and 17—lake) identification, and (**c**) zoom-in for the five locations of urban parks and the lake.

Parks 1 and 3 are in a mixed area of urban and rural land use. The surroundings have close low-rise buildings (class 33) in the northwest part and scattered buildings with undergrowth and trees (class 39) in the southeast region, representing rural settlements. Park 2 is in a transition area between the compact low-rise (33) and heavy industry (40) land use classes. Parks 4 and 5 have the most diverse boundary areas, ranging between classes with low numbers of dwellings (sparsely low-rise, 39) and compact high-rise (31), which are characterized by the high density of tall buildings and low or no presence of vegetation.

To evaluate the influence of LCZ, Table S4 shows the index performance by supplementary results in simulations (d03) using the default land use (DEFAULT simulation) and implemented urban LCZ classes (SA simulation) for stations with data available. The SA simulation showed significant improvement in the representation of meteorological variables, especially in the reproduction of wind speed values for the IAT station over the DEFAULT simulation. Despite the clearly large difference between the simulated and observed data, this is due to the fact that wind is a difficult variable to capture in mesoscale models as a function of its strong interactivity with the varied components that comprise the urban system [78,79].

This better representation at this station is associated with the improvement in urban morphology at this point by using LCZ (e.g., considering the height of the building) in the SA simulation. Similar results were obtained by enhanced model representation for T2 and WS10, since LCZs lead to the representation of urban structures [80–82]. However, to effectively improve Q2 values, it is recommended to include parameterizations to represent the urban vegetation [83,84].

Figure 3 shows the comparison between observed and simulated values in SB (considered here as a reference to compare with the observations) for IAT and SIMEPAR stations (T2, Q2, and WS10) from September 6 to 16, 2017. Table 4 shows the statistical performance of the model.

The model presented adequate temporal representation of T2, r = 0.95 in both the IAT and SIMEPAR stations, indicating a strong correlation between predicted and observed values. For Q2, r = 0.49 in IAT and r = 0.43 in SIMEPAR (weak correlation) were obtained. MB values indicated the most significant deviations in the SIMEPAR station for T2 (1.84 °C) and WS10 (-0.75 m.s^{-1}). The S_{Pielke} provides an effective representation for T2 in both stations.

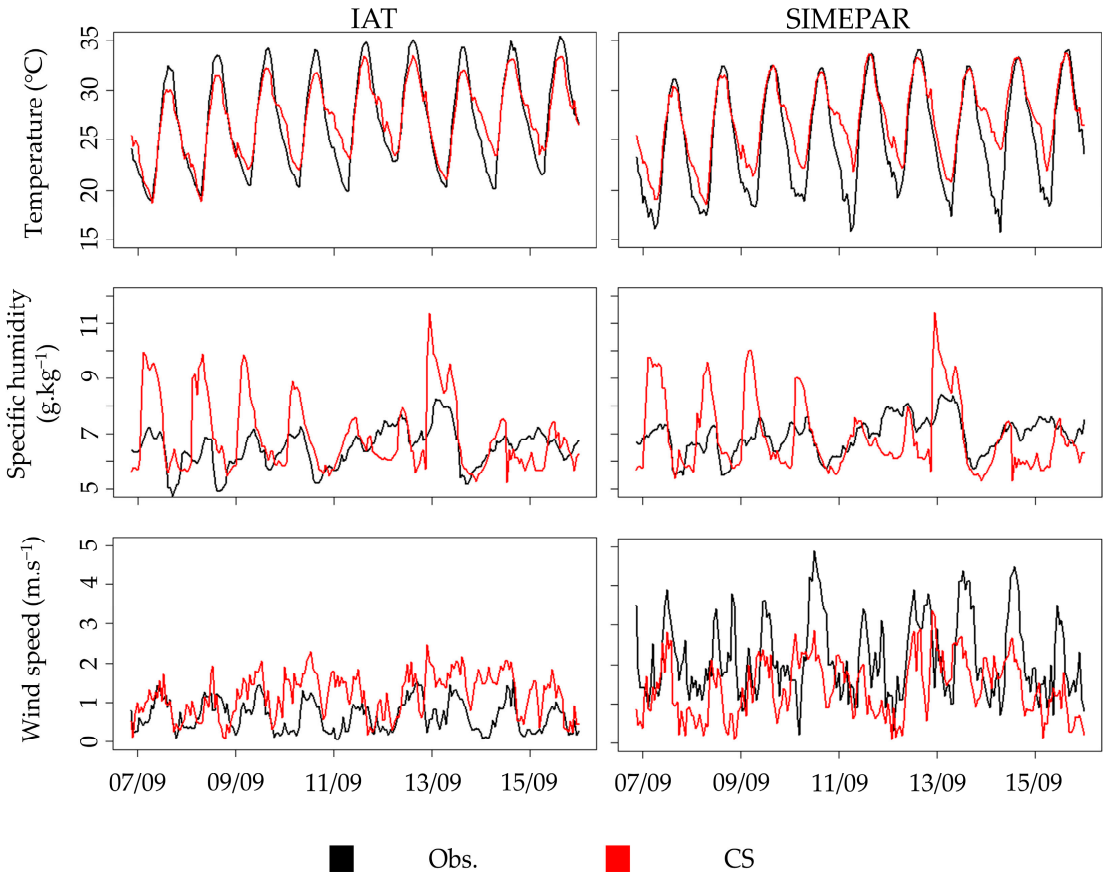

Figure 3. Temporal evaluation of T2, Q2, and WS10 simulated (red) and observed (black) for IAT and SIMEPAR.

Table 4. Statistical performance for meteorological variables estimated in SB (d04).

Variable	Station	$Mean_{obs}$	$Mean_{sim}$	σ_{obs}	σ_{sim}	r	MB	RMSE	S_{Pielke}
T2 (°C)	IAT	26.99	27.15	4.75	3.66	0.95	0.16	1.69	1.00
	SIMEPAR	25.19	27.04	5.30	3.86	0.95	1.84	2.75	1.02
Q2 ($g.kg^{-1}$)	IAT	6.49	6.93	0.70	1.31	0.49	0.44	1.22	3.19
	SIMEPAR	6.94	6.93	0.65	1.30	0.43	−0.02	1.18	3.75
WS10 ($m.s^{-1}$)	IAT	0.65	1.18	0.40	0.55	0.35	0.53	0.77	2.75
	SIMEPAR	2.15	1.41	1.01	0.75	0.42	−0.75	1.22	4.10

3.2. Urban Lake

The effects of the artificial Londrina urban lake were assessed by analyzing the T2 and Q2 simulated values around the lake (Figure 4), i.e., comparing simulations SA with SB by the differential percentage (corresponding to ((SB-SA)/SB) × 100), where positive values indicate that the simulated values in SB were higher in the presence of the lake, and negative values indicate that the simulated values in SB were lower in the presence of the lake. Weather contributions were evaluated for the highly impervious urban classes with few or no trees (classes 31, 32, and 33).

Comparing the differences between SB and SA (without the lake), there was a minimal contribution to the temporal percentage difference evolution of Q2 in the three points analyzed around the lake, prevailing the reduction in specific humidity. However, nighttime T2 at the three points indicates the effect of increasing temperatures by up to 5%, while a slight decrease was observed during the day.

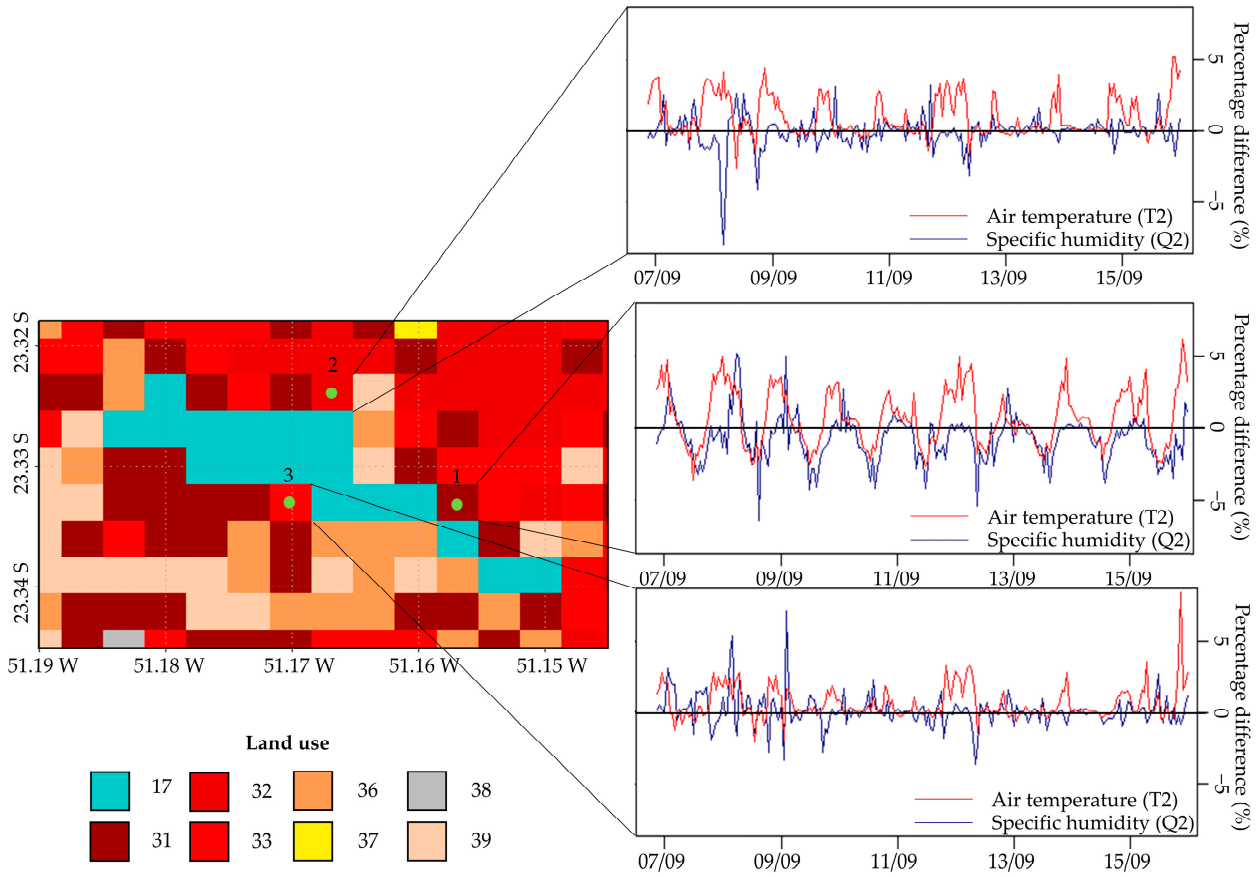

Figure 4. Superficial area of the lake (class 17), urban areas (classes 31 to 39, Figure 2), and difference in the percentage of T2 and Q2 between SB and SA at three points around the lake (graphics).

These results are corroborated by Jacobs et al. [85] and explained by the thermal inertia and high heat capacity of water [86]. During the night, the cooling effect weakens and becomes a warming effect due to the air temperature becoming lower than the water temperature. At that point, the water body begins to warm the surrounding area [87]. Moreover, the lake breeze frequency declines as the dimensions of water bodies decrease [88]. In contrast, the circulation on a smaller scale (lake breeze) can be reduced by the surface [89]. These effects of urban lakes are pointed to be smaller in autumn and winter [90].

Overall, our results indicate a smooth effect of the urban lake on Q2 and T2 (with opposite contributions during day and night). Therefore, this type of GI (small urban lake) does not significantly influence the weather conditions around of lake and brings benefits to mitigate the UHI, corroborated by measurements performed in loco in the same region where no clear relationship was identified between the decrease in UHI intensity and the fraction of water bodies [91].

Therefore, these findings suggest that the implementation of urban lakes for the exclusive purpose of mitigating the effects of urbanization on air humidity and temperature is not appropriate. However, it is important to note that the lake area and its surroundings benefit the inhabitants, since they are the main outdoor activities, recreation, and leisure [92–96].

3.3. Urban Parks

To evaluate the effects of urban parks on the meteorological variables, we analyzed the simulation results of SC to SA at and around urban parks and at the surface and vertical levels. The results are presented for urban parks 1 (UP1) and 4 (UP4) in the main text, and others are in the Supplementary Material. Figure 5 and Figure S2 show the simulated values in the urban parks.

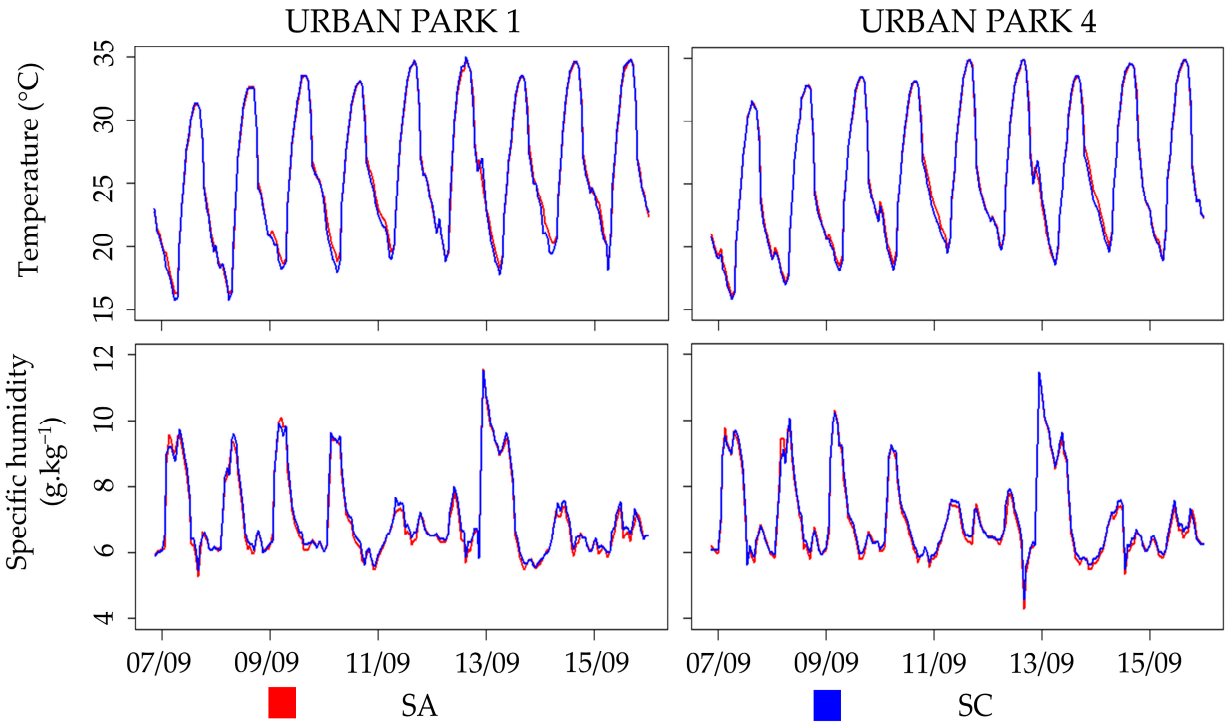

Figure 5. Temporal evaluation of temperature and specific humidity simulated at UP1 and UP4. The red line is the data by SA, while the blue line represents the data by SC.

In Figure 5, it was not possible to observe significant differences between the maximum values of T2 and Q2, comparing SA and SB. However, the minimum values were lower for T2 and higher for Q2. The average of T2 decreases by 0.14 °C in UP1 and 0.13 °C in UP4, while the mean of Q2 increases by 1.24 % (UP1) and 1.04 % (UP4). The T2 daily average minimum values were reduced by 3.00 % in UP1 and 1.74 % in UP4. However, the same reduction in T2 did not occur in the daily average maximum values, as the entire surface is heated homogeneously by solar radiation, corroborating the data obtained by Papangelis et al. [97]. The cooling rates are due to the park characteristics, since they lead to evapotranspiration and have small heat storage compared to urban structures, resulting in lower air temperature [21,98].

Given the importance of urban canyon physical, thermal, and radiative properties of the surfaces in the effect of UHI intensity [99,100], an analysis of the surface energy budget must be carried out, particularly the sensible and latent heat fluxes. The increase in water vapor through evapotranspiration directly influences the surface energy fluxes (Figures 6 and S3). The latent heat flux increased by 370 % in UP1 due to the increased Q2, as most of the available energy on the surface dissipated to the water vapor phase change. The change of urban classes by GIs lead to a 2.80 % reduction in the sensible heat flux in UP4, since more green areas are available in this simulation [83]. However, the same reduction did not occur in UP1, since the same area consists of underbrush in the SB simulation, which can already be considered a green area. In this case, the increase observed in the sensible heat flux with high vegetation can be associated with the stored ground heat flux, which dissipates more heat to the air [101]. Situations like this can contribute to the increase in UHI intensity even with the presence of green areas, mainly as a function of the LCZ near the parks, which can retain most of the solar radiation in the canyon formed by vegetation, and the intensity of UHI increases with other factors, such as season length for tropical areas [6,102].

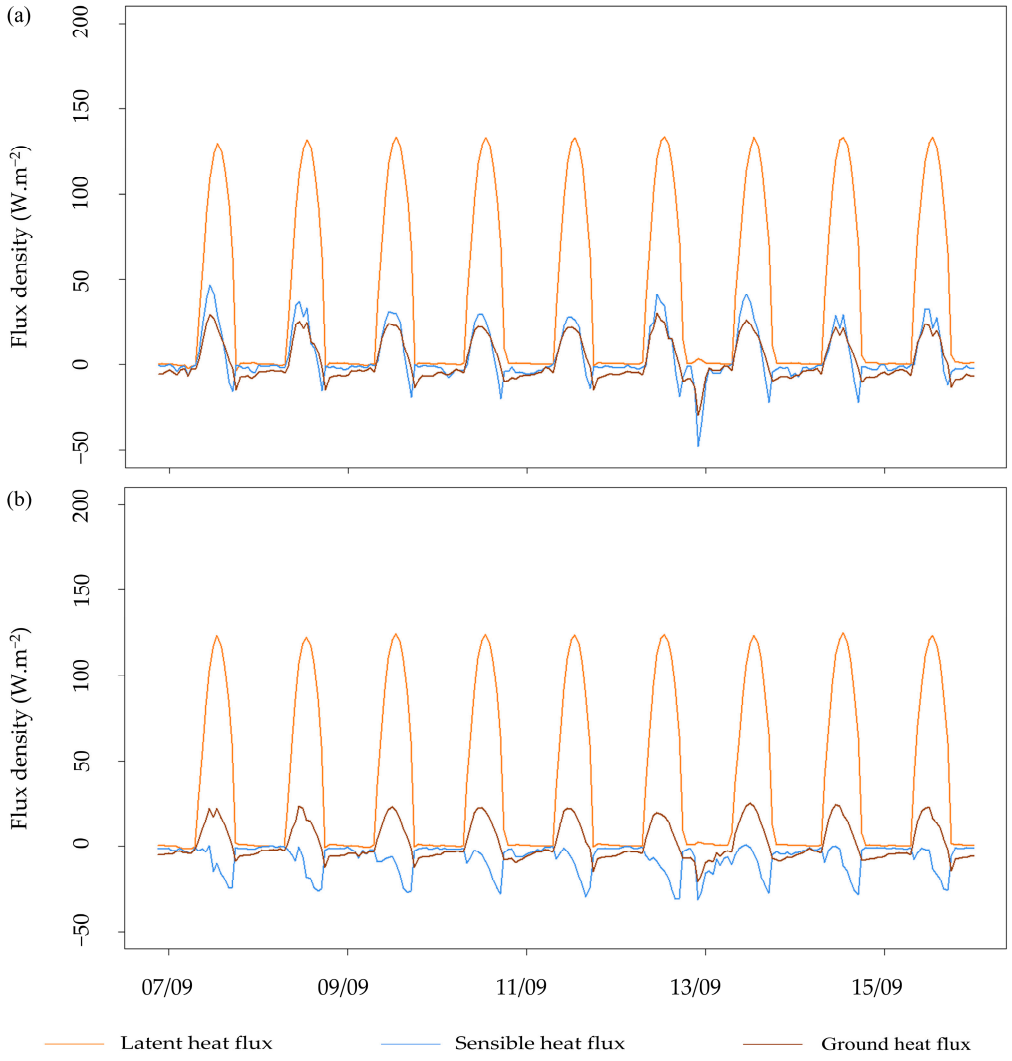

Figure 6. Diurnal difference (SC–SA) of simulated surface energy fluxes (W.m^{-2}) at (**a**) UP1 and (**b**) UP4.

A sudden drop in sensible heat fluxes and ground heat was recorded at the end of the day on September 12, 2017, which can be explained by a change in the temperature profile between 19:00 and 21:00, as shown in Figure S4. In the SA simulation, where the lake is changed for the LCZ, the implementation of the urban area increases the energy storage capacity due to the thermal properties of building materials [100]. Those materials re-emit that energy by the longwave radiation during nighttime, which can enhance UHI intensity [97].

The temporal evolution of cooling/warming rates in UP1 and UP4 was similar to heating rates after sunrise (6:30) and cooling rates in the nighttime, after sunset (18:15). Greater intensities were found between 7:00 p.m. and 6:00 a.m. (Figures 7 and S5).

Urban parks play an important role in cooling the air, especially at nighttime. Although the temporal evolution and the vegetation characteristics are similar in both parks, UP1 has an area twice as large as UP4, 8.00 km^2 and 4.00 km^2, respectively (Table S2). These aspects are directly related to more intense cooling rates in UP1 than UP4, especially between midnight and 7:00 a.m.

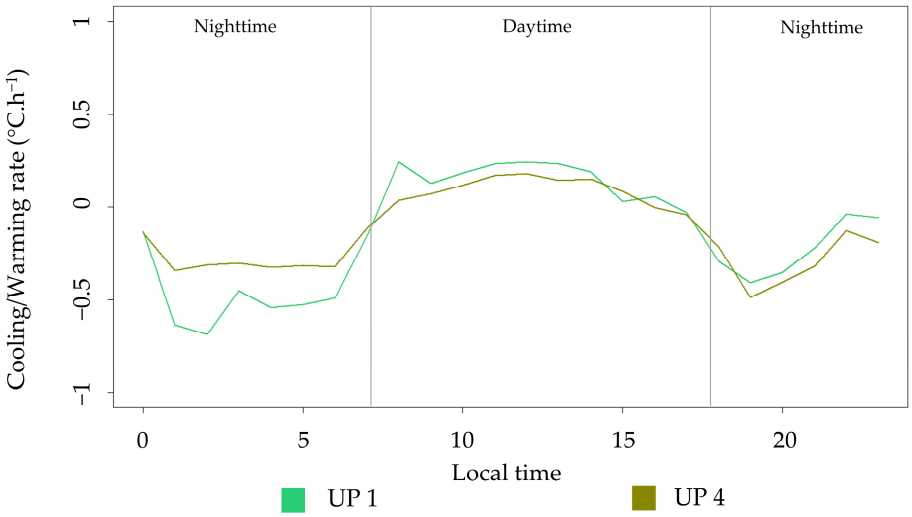

Figure 7. Diurnal cooling/warming rates (°C.h^{-1}) calculated from SA and SB simulations at UP1 and UP4. Note: heating/cooling rate is the difference between SB and SA of the simulated T2 (SC–SA).

Figure 8 presents the spatialized 3 h average cooling/warming rates between 7:00 p.m. and 6:00 a.m. Rated cooling along the grid was 0.5 °C.h^{-1} inside the park upper to 5.0 °C.h^{-1}, and the highest average contribution in the period was from 3:00 to 5:00 a.m. The simulation results in Figure 8 show up to 2 km positive contribution in T2. The vegetation increase is the most effective strategy in mitigating extreme urban temperatures since it encompasses a more extensive area than other mitigation projects, such as the rise of surface albedo or architectural shading [13].

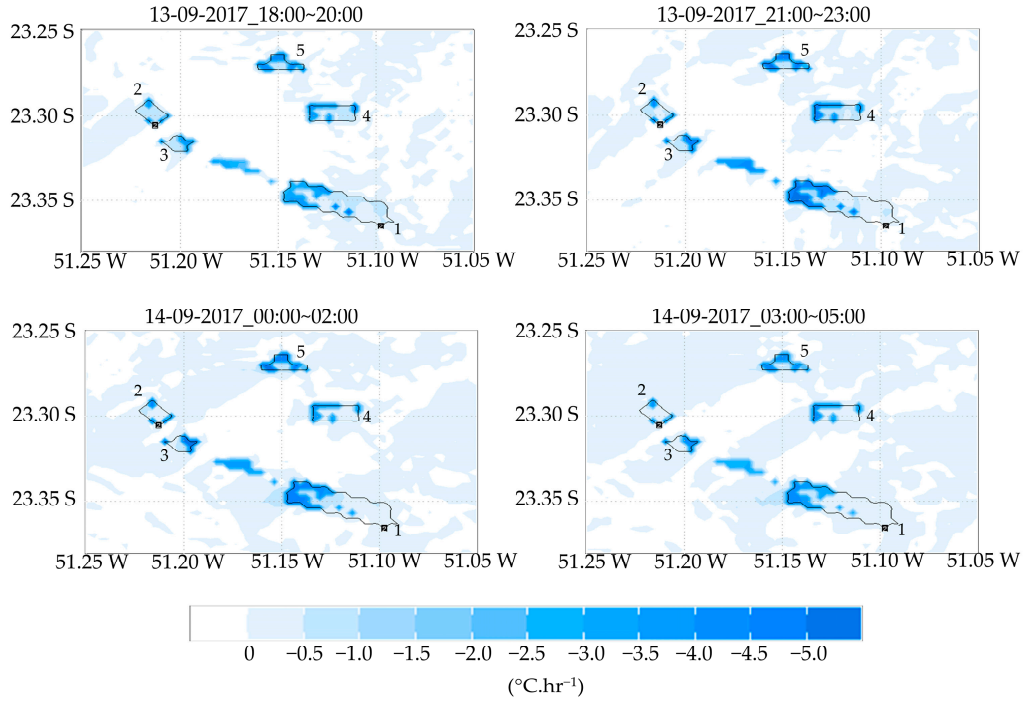

Figure 8. Mean spatial differences (SC–SA) of T2 temperatures (°C.h^{-1}) during nighttime (September 13th to 14th). A more detailed map is shown in Figure S6. Note: Urban delimitation of Londrina (red outline) and parks (black outline).

It is essential to emphasize that, in addition to the visual benefit that these environmental structures provide to the local community, they cause effects that mitigate UHI and improve outdoor thermal comfort. Urban parks directly influence air temperature

reduction, surface solar radiation, and increased humidity, developing a local microclimate and improved thermal sensation [12,103–106].

Vegetation has a higher friction factor of the wind vector components than urban structures, hindering vertical and horizontal dispersion of air pollutants. This impact can be seen in Figure 9, when comparing the vertical and zonal wind components and specific humidity in the simulations without and with the park identification SA and SC, respectively.

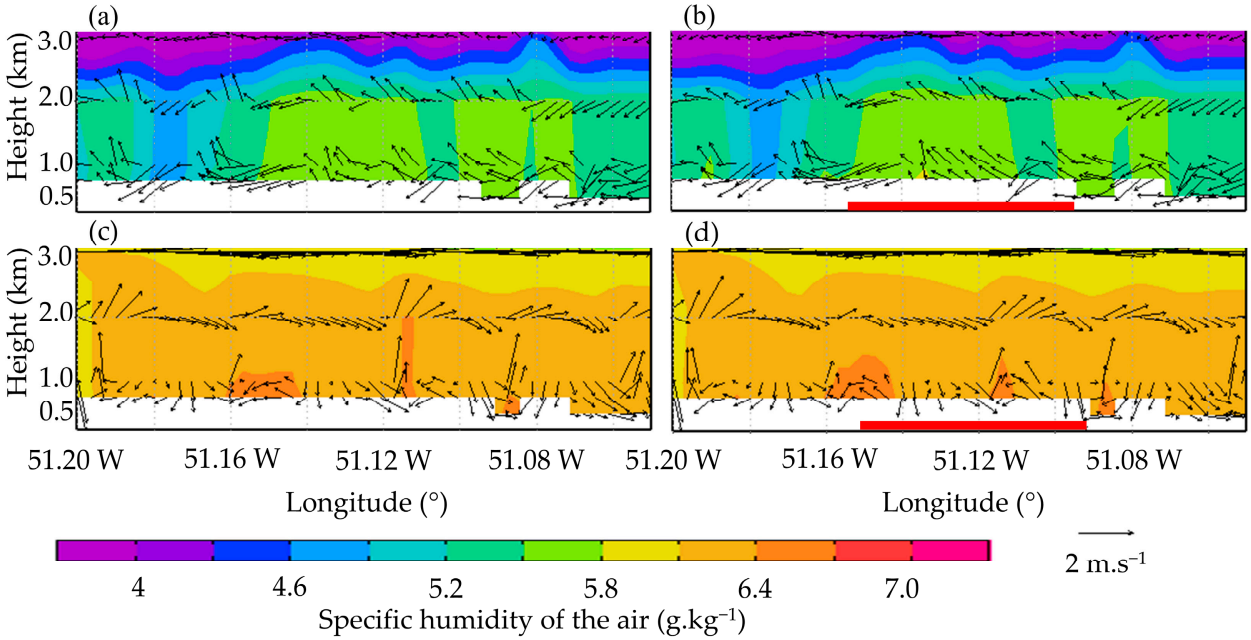

Figure 9. Specific air humidity (g.kg^{-1}), vertical and zonal component of the wind (m.s^{-1}) for UP 1 at 23.35° S. Note: (**a**,**b**) results without and with UP1 for 15:00 on 9 July 2017, respectively; (**c**,**d**) results without and with UP1 for 12:00 on 9 August 2017, respectively. The red line represents the longitudinal dimension of UP1.

The drag effect in wind speed results in a lower intensity of the convective processes near the UP1 area, including a decrease in the vertical mixing process and lower boundary layer depth. Reduced wind speed and decreased vertical mixing during the day can lead to stagnation of air near the surface [107]. The higher friction factor of the wind by the vegetation can lead to greater retention of pollutants in the air masses. Thus, the foliage can assist in removing part of the pollutants [26,108,109].

To summarize, the comparison of the model results showed that the existing urban lake in MAL has little impact on mesoscale meteorology (SA versus SB). In contrast, urban parks (SA vs. SC) can be an effective natural solution for mitigating the effects of urbanization on meteorological variables such as the UHI, even in a medium-sized city.

In this sense, cities must be prepared for such an expansion process, considering GIs' inclusion in the development of Master Plans to minimize the climate impacts of urbanization [30,110,111], besides the other benefits recognized [31,112–114]. Furthermore, it is worth noting that implementing these infrastructures in small- and medium-sized urbanization affects a smaller number of people due to the relocation of the population and demands less financial investment in execution as they are preventive actions [115,116]. Therefore, our results demonstrated the benefits of green parks even in the urban atmosphere of a medium-sized city and the importance of studies to evaluate the use of GIs, considering the local urban characteristics and climate.

4. Conclusions and Remarks

Numerical simulations were performed using the WRF model for MAL, Brazil, considering the improvement in urban land representation, to study the effects on the urban atmosphere due to added GIs on the urban landscape.

Using the urban LCZ classes has proven to be an effective way to represent the urban impact on meteorological variables, particularly in the wind speed, even being a complex variable to simulate. It is because the LCZ representation can accurately depict the various urban structures and their impact on local weather patterns. As a result, adopting LCZ classes has greatly improved the modeling of meteorological phenomena in urban environments by the WRF.

Recognizing the limitations of analysis by using numerical simulations, the results of SB indicate cooling effects and higher specific humidity along the d04 grid, showing higher intensities (up to -5 °C.h^{-1} for T2) within GI (park) during calm conditions in the nighttime. Blue GI (lake) did not present relevant effects on the analyzed variables.

Our results demonstrate that the GIs (parks) play an essential role since, in addition to causing soil shading, they absorb solar energy, preventing UHI. The GI directly influences heat flux in the soil, reducing the maximum intensity of sensitive heat (2.80%) and increasing the maximum latent heat flux (368%). Urban parks were distributed homogeneously throughout urban areas, favoring their benefits along the city, and allocated in areas with less population density and with remaining vegetation. Furthermore, it is important to emphasize that these results are for relatively small green parks placed outside downtown (higher urbanization) and a medium-sized city, which tends to grow, like many others in the world.

These results provide information on GIs' meteorological contributions, highlighting the benefits of increasing urban vegetation to mitigate atmospheric urbanization effects even in smaller urban areas. Thus, our findings are useful, supporting public decision-makers in developing Master Plans in medium-sized cities. Finally, we believe that the intelligent reconciliation of human beings with nature is the way to increase the resilience of urban areas and mitigate the impacts of urbanization. Thus, the implementation of urban vegetation, after previous studies, must be expanded in scope and intensity, particularly in developing cities.

Supplementary Materials: The following supporting information can be downloaded at: https://www.mdpi.com/article/10.3390/su15021429/s1, Figure S1: (a) SIMEPAR and (b) IAT monitoring station; Figure S2: Temporal evaluation of temperature and specific humidity simulated at urban parks 2, 3, and 5; Figure S3: Diurnal difference (SC-SA) of simulated surface energy fluxes (W.m^{-2}) at (a) UP 2, (b) UP3, and (c) UP5; Figure S4: Diurnal cooling/warming rates (°C.h^{-1}) calculated from the SA and SC simulations compared to rates calculated from hourly air temperature observations at UP2, UP3, and UP5; Figure S5: Mean spatial differences (SC–SA) of T2 temperatures (°C.h^{-1}) during nighttime (September 13th to 14th); Table S1: Characteristics of LCZ urban classes; Table S2: Dimensions of urban GIs (lake and parks); Table S3: Accuracy Matrix for MAL WUDAPT Level "0", with known (vertical axis) vs. predicted (horizontal axis) test-class frequencies; Table S4: Statistical performance of simulations for meteorological variables at domain d03.

Author Contributions: Conceptualization, O.M.S., M.V.B.d.M., and L.D.M.; Data curation, O.M.S.; Funding acquisition, M.V.B.d.M. and L.D.M.; Investigation, O.M.S.; Methodology, O.M.S., A.P.R., M.V.B.d.M., and L.D.M.; Project administration, M.V.B.d.M. and L.D.M.; Resources, M.V.B.d.M. and L.D.M.; Software, M.V.B.d.M.; Supervision, M.V.B.d.M. and L.D.M.; Validation, O.M.S.; Visualization, O.M.S., A.P.R., M.V.B.d.M., and L.D.M.; Writing—original draft, O.M.S.; Writing—review and editing, A.P.R., M.V.B.d.M., and L.D.M. All authors have read and agreed to the published version of the manuscript.

Funding: This study was supported by CNPq (Conselho Nacional de Desenvolvimento Científico e Tecnológico, processes 436466/2018-0 and 380558/2019-0) and by ANID (Agencia Nacional del Investigación y Desarrollo) Fondecyt Iniciación N° 11220138.

Institutional Review Board Statement: Not applicable.

Informed Consent Statement: Not applicable.

Data Availability Statement: Not applicable.

Acknowledgments: The authors would like to thank the IAT (Instituto Água e Terra) and SIMEPAR (Sistema de Tecnologia e Monitoramento Ambiental do Paraná) for providing the meteorological data.

Conflicts of Interest: All authors declare no conflict of interest about the representation or interpretation of reported research results.

References

1. Borras, S.M.; Franco, J.C.; Nam, Z. Climate Change and Land: Insights from Myanmar. *World Dev.* **2020**, *129*, 104864. [CrossRef]
2. Austin, E.K.; Rich, J.L.; Kiem, A.S.; Handley, T.; Perkins, D.; Kelly, B.J. Concerns about Climate Change among Rural Residents in Australia. *J. Rural. Stud.* **2020**, *75*, 98–109. [CrossRef]
3. De Oliveira, J.V.; Cohen, J.C.P.; Pimentel, M.; Tourinho, H.L.Z.; Lôbo, M.A.; Sodré, G.; Abdala, A. Urban Climate and Environmental Perception about Climate Change in Belém, Pará, Brazil. *Urban Clim.* **2020**, *31*, 100579. [CrossRef]
4. Zhang, C.; Wang, X.; Li, J.; Hua, T. Identifying the Effect of Climate Change on Desertification in Northern China via Trend Analysis of Potential Evapotranspiration and Precipitation. *Ecol. Indic.* **2020**, *112*, 106141. [CrossRef]
5. De Morais, M.V.B.; Freitas, E.; Marciotto, E.; Guerrero, V.; Martins, L.; Martins, J. Implementation of Observed Sky-View Factor in a Mesoscale Model for Sensitivity Studies of the Urban Meteorology. *Sustainability* **2018**, *10*, 2183. [CrossRef]
6. De Morais, M.V.B.; Guerrero, V.V.U.; Martins, L.D.; Martins, J.A. Dynamical Downscaling of Future Climate Change Scenarios in Urban Heat Island and Its Neighborhood in a Brazilian Subtropical Area. *Proc. West. Mark. Ed. Assoc. Conf.* **2017**, *1*, 106. [CrossRef]
7. Mohajerani, A.; Bakaric, J.; Jeffrey-Bailey, T. The Urban Heat Island Effect, Its Causes, and Mitigation, with Reference to the Thermal Properties of Asphalt Concrete. *J. Environ. Manag.* **2017**, *197*, 522–538. [CrossRef]
8. Hu, Y.; Jia, G.; Pohl, C.; Zhang, X.; van Genderen, J. Assessing Surface Albedo Change and Its Induced Radiation Budget under Rapid Urbanization with Landsat and GLASS Data. *Theor. Appl. Climatol.* **2016**, *123*, 711–722. [CrossRef]
9. Oke, T. The Energetic Basis of Urban Heat Island. *Q. J. Royal Meteorol. Soc.* **1982**, *108*, 1–24. [CrossRef]
10. Mölders, N. Land-Use and Land-Cover Changes: Impact on Climate and Air Quality. *Land.-Use. Land.-Cover. Chang.* **2011**, *44*. [CrossRef]
11. Gago, E.J.; Roldan, J.; Pacheco-Torres, R.; Ordóñez, J. The City and Urban Heat Islands: A Review of Strategies to Mitigate Adverse Effects. *Renew. Sustain. Energy Rev.* **2013**, *25*, 749–758. [CrossRef]
12. Chan, S.Y.; Chau, C.K.; Leung, T.M. On the Study of Thermal Comfort and Perceptions of Environmental Features in Urban Parks: A Structural Equation Modeling Approach. *Build. Env.* **2017**, *122*, 171–183. [CrossRef]
13. McRae, I.; Freedman, F.; Rivera, A.; Li, X.; Dou, J.; Cruz, I.; Ren, C.; Dronova, I.; Fraker, H.; Bornstein, R. Integration of the WUDAPT, WRF, and ENVI-Met Models to Simulate Extreme Daytime Temperature Mitigation Strategies in San Jose, California. *Build. Env.* **2020**, *184*, 107180. [CrossRef]
14. Giannaros, C.; Nenes, A.; Giannaros, T.M.; Kourtidis, K.; Melas, D. A Comprehensive Approach for the Simulation of the Urban Heat Island Effect with the WRF/SLUCM Modeling System: The Case of Athens (Greece). *Atmos. Res* **2018**, *201*, 86–101. [CrossRef]
15. Niu, G.-Y.; Yang, Z.-L.; Mitchell, K.E.; Chen, F.; Ek, M.B.; Barlage, M.; Kumar, A.; Manning, K.; Niyogi, D.; Rosero, E.; et al. The Community Noah Land Surface Model with Multiparameterization Options (Noah-MP): 1. Model Description and Evaluation with Local-Scale Measurements. *J. Geophys. Res. Atmos.* **2011**, *116*, 015139. [CrossRef]
16. Pappaccogli, G.; Giovannini, L.; Zardi, D.; Martilli, A. Sensitivity Analysis of Urban Microclimatic Conditions and Building Energy Consumption on Urban Parameters by Means of Idealized Numerical Simulations. *Urban Clim.* **2020**, *34*, 100677. [CrossRef]
17. Ghofrani, Z.; Sposito, V.; Faggian, R. A Comprehensive Review of Blue-Green Infrastructure Concepts. *Int. J. Environ. Sustain.* **2017**, *6*, 15–36. [CrossRef]
18. World Health Organization. Urban Green Spaces: A Brief for Action. *Reg. Off. Eur.* **2017**, *24*, 2–3.
19. De Morais, M.V.B.; Guerrero, V.V.U. Analysis of Computational Performance and Adaptive Time Step for Numerical Weather Prediction Models. *Int. J. Eng. Math. Model.* **2018**, *2018*, 1–8.
20. De Munck, C.S.; Lemonsu, A.; Bouzouidja, R.; Masson, V.; Claverie, R. The GREENROOF Module (v7.3) for Modelling Green Roof Hydrological and Energetic Performances within TEB. *Geosci. Model. Dev* **2013**, *6*, 1941–1960. [CrossRef]
21. Li, X.X.; Norford, L.K. Evaluation of Cool Roof and Vegetations in Mitigating Urban Heat Island in a Tropical City, Singapore. *Urban Clim.* **2016**, *16*, 59–74. [CrossRef]
22. Rafael, S.; Vicente, B.; Rodrigues, V.; Miranda, A.I.; Borrego, C.; Lopes, M. Impacts of Green Infrastructures on Aerodynamic Flow and Air Quality in Porto's Urban Area. *Atmos. Env.* **2018**, *190*, 317–330. [CrossRef]
23. Tiwari, A.; Kumar, P.; Kalaiarasan, G.; Ottosen, T.-B. The Impacts of Existing and Hypothetical Green Infrastructure Scenarios on Urban Heat Island Formation. *Environ. Pollut.* **2021**, *274*, 115898. [CrossRef] [PubMed]
24. Vos, P.E.J.; Maiheu, B.; Vankerkom, J.; Janssen, S. Improving Local Air Quality in Cities: To Tree or Not to Tree? *Environ. Pollut.* **2013**, *183*, 113–122. [CrossRef] [PubMed]

25. Wang, C.; Li, Q.; Wang, Z.H. Quantifying the Impact of Urban Trees on Passive Pollutant Dispersion Using a Coupled Large-Eddy Simulation–Lagrangian Stochastic Model. *Build. Env.* **2018**, *145*, 33–49. [CrossRef]
26. Abhijith, K.V.; Kumar, P.; Gallagher, J.; McNabola, A.; Baldauf, R.; Pilla, F.; Broderick, B.; di Sabatino, S.; Pulvirenti, B. Air Pollution Abatement Performances of Green Infrastructure in Open Road and Built-up Street Canyon Environments–A Review. *Atmos. Env.* **2017**, *162*, 71–86. [CrossRef]
27. Tiwari, A.; Kumar, P.; Baldauf, R.; Zhang, K.M.; Pilla, F.; di Sabatino, S.; Brattich, E.; Pulvirenti, B. Considerations for Evaluating Green Infrastructure Impacts in Microscale and Macroscale Air Pollution Dispersion Models. *Sci. Total. Environ.* **2019**, *672*, 410–426. [CrossRef]
28. Vogt, J.; Hauer, R.; Fischer, B. The Costs of Maintaining and Not Maintaining the Urban Forest: A Review of the Urban Forestry and Arboriculture Literature. *Arboric. Urban For.* **2015**, *41*, 293–323. [CrossRef]
29. Liberalesso, T.; Oliveira Cruz, C.; Matos Silva, C.; Manso, M. Green Infrastructure and Public Policies: An International Review of Green Roofs and Green Walls Incentives. *Land Use Policy* **2020**, *96*, 104693. [CrossRef]
30. Choi, C.; Berry, P.; Smith, A. The Climate Benefits, Co-Benefits, and Trade-Offs of Green Infrastructure: A Systematic Literature Review. *J. Environ. Manag.* **2021**, *291*, 112583. [CrossRef]
31. Zeng, J.; Lin, G.; Huang, G. Evaluation of the Cost-Effectiveness of Green Infrastructure in Climate Change Scenarios Using TOPSIS. *Urban For. Urban Green.* **2021**, *64*, 127287. [CrossRef]
32. Anjos, M.; Targino, A.C.; Krecl, P.; Oukawa, G.Y.; Braga, R.F. Analysis of the Urban Heat Island under Different Synoptic Patterns Using Local Climate Zones. *Build. Env.* **2020**, *185*, 107268. [CrossRef]
33. United Nations Department of Economic and Social Affairs. *Population Division. World Urbanization Prospects: The 2018 Revision (ST/ESA/SER.A/420) 2019*; United Nations Department of Economic and Social Affairs: New York, NY, USA, 2019.
34. Targino, A.C.; Krecl, P.; Coraiola, G.C. Effects of the Large-Scale Atmospheric Circulation on the Onset and Strength of Urban Heat Islands: A Case Study. *Theor. Appl. Climatol.* **2014**, *117*, 73–87. [CrossRef]
35. Shackleton, C.M.; Blair, A.; de Lacy, P.; Kaoma, H.; Mugwagwa, N.; Dalu, M.T.; Walton, W. How Important Is Green Infrastructure in Small and Medium-Sized Towns? Lessons from South Africa. *Landsc. Urban Plan.* **2018**, *180*, 273–281. [CrossRef]
36. IBGE-Instituto Brasileiro de Geografia e Estatística. *Censo Demográfico: Características Da População–Amostra 2019*; IBGE-Instituto Brasileiro de Geografia e Estatística: Rio de Janeiro, RJ, Brazil, 2019.
37. González, C.M.; Ynoue, R.Y.; Vara-Vela, A.; Rojas, N.Y.; Aristizábal, B.H. High-Resolution Air Quality Modeling in a Medium-Sized City in the Tropical Andes: Assessment of Local and Global Emissions in Understanding Ozone and PM10 Dynamics. *Atmos. Pollut. Res.* **2018**, *9*, 934–948. [CrossRef]
38. Cardoso, R.D.S.; Dorigon, L.P.; Teixeira, D.C.F.; Amorim, M.C.D.C.T. Assessment of Urban Heat Islands in Small- and Mid-Sized Cities in Brazil. *Climate* **2017**, *5*, 14. [CrossRef]
39. Saide, P.E.; Mena-Carrasco, M.; Tolvett, S.; Hernandez, P.; Carmichael, G.R. Air Quality Forecasting for Winter-Time PM2.5 Episodes Occurring in Multiple Cities in Central and Southern Chile. *J. Geophys. Res. Atmos.* **2016**, *121*, 558–575. [CrossRef]
40. Arghavani, S.; Malakooti, H.; Bidokhti, A.A. Evaluation the Effects of Urban Green Space Scenarios on Near-Surface Turbulence and Dispersion Related Parameters: A Numerical Case Study in Tehran Metropolis. *Urban For. Urban Green.* **2021**, *59*, 127012. [CrossRef]
41. Li, D.; Bou-Zeid, E.; Oppenheimer, M. The Effectiveness of Cool and Green Roofs as Urban Heat Island Mitigation Strategies. *Environ. Res. Lett.* **2014**, *9*, 55002. [CrossRef]
42. Capucim, M.N.; Brand, V.S.; Machado, C.B.; Martins, L.D.; Allasia, D.G.; Homann, C.T.; de Freitas, E.D.; Dias, M.A.F.; Andrade, M.F.; Martins, J.A. South America Land Use and Land Cover Assessment and Preliminary Analysis of Their Impacts on Regional Atmospheric Modeling Studies. *IEEE J. Sel. Top. Appl. Earth. Obs. Remote Sens.* **2015**, *8*, 1185–1198. [CrossRef]
43. Rudke, A.P.; Fujita, T.; de Almeida, D.S.; Eiras, M.M.; Xavier, A.C.F.; Rafee, S.A.A.; Santos, E.B.; de Morais, M.V.B.; Martins, L.D.; de Souza, R.V.A.; et al. Land Cover Data of Upper Parana River Basin, South America, at High Spatial Resolution. *Int. J. Appl. Earth Obs. Geoinformation* **2019**, *83*, 101926. [CrossRef]
44. Chen, X.; Xu, Y.; Yang, J.; Wu, Z.; Zhu, H. Remote Sensing of Urban Thermal Environments within Local Climate Zones: A Case Study of Two High-Density Subtropical Chinese Cities. *Urban Clim.* **2020**, *31*, 100568. [CrossRef]
45. Zheng, Y.; Ren, C.; Xu, Y.; Wang, R.; Ho, J.; Lau, K.; Ng, E. GIS-Based Mapping of Local Climate Zone in the High-Density City of Hong Kong. *Urban Clim.* **2018**, *24*, 419–448. [CrossRef]
46. Köppen, W. Klassifikation Der Klimate Nach Temperatur, Niederschlag Und Jahreslauf. *Petermanns Geogr. Mitt.* **1918**, *64*, 193–203.
47. National Institute of Meteorology-Brazil. *Climate. Normal. (1991/2020)*; National Institute of Meteorology-Brazil: Brasilia, Brazil, 2022.
48. Grell, G.A.; Peckham, S.E.; Schmitz, R.; McKeen, S.A.; Frost, G.; Skamarock, W.C.; Eder, B. Fully Coupled "Online" Chemistry within the WRF Model. *Atmos. Environ.* **2005**, *39*, 6957–6975. [CrossRef]
49. Mottaghi, S.; Gabbai, R.; Benaroya, H. *An Analytical Mechanics Framework for Flow-Oscillator Modeling of Vortex-Induced Bluff-Body Oscillations*, 1st ed.; Springer: Cham, Switzerland, 2020; ISBN 978-3-030-26131-3.
50. Franco, D.M.P.; de Andrade, M.F.; Ynoue, R.Y.; Ching, J. Effect of Local Climate Zone (LCZ) Classification on Ozone Chemical Transport Model Simulations in Sao Paulo, Brazil. *Urban Clim.* **2019**, *27*, 293–313. [CrossRef]

51. Gavidia-Calderón, M.; Vara-Vela, A.; Crespo, N.M.; Andrade, M.F. Impact of Time-Dependent Chemical Boundary Conditions on Tropospheric Ozone Simulation with WRF-Chem: An Experiment over the Metropolitan Area of São Paulo. *Atmos. Environ.* **2018**, *195*, 112–124. [CrossRef]
52. Hoshyaripour, G.; Brasseur, G.; Andrade, M.F.; Gavidia-Calderón, M.; Bouarar, I.; Ynoue, R.Y. Prediction of Ground-Level Ozone Concentration in São Paulo, Brazil: Deterministic versus Statistic Models. *Atmos. Environ.* **2016**, *145*, 365–375. [CrossRef]
53. Martins, L.D.; Vidotto, L.H.B.; de Ameida, D.S.; Squizatto, R.; Moreira, C.A.B.; Capucim, M.N.; Martins, J.A. The Role of Medium-Sized Cities for Global Tropospheric Ozone Levels. *Energy Procedia* **2016**, *95*, 265–271. [CrossRef]
54. Vara-Vela, A.; Andrade, M.F.; Kumar, P.; Ynoue, R.Y.; Muñoz, A.G. Impact of Vehicular Emissions on the Formation of Fine Particles in the Sao Paulo Metropolitan Area: A Numerical Study with the WRF-Chem Model. *Atmos. Chem. Phys.* **2016**, *16*, 777–797. [CrossRef]
55. National Weather Service Centers for Environmental Prediction. *Department, O.C.S. NCEP GDAS/FNL 0.25 Degree Global Tropospheric Analyses and Forecast Grids 2015*; National Weather Service Centers for Environmental Prediction: College Park, MD, USA, 2015.
56. Chou, M.-D.; Suarez, M. A Solar Radiation Parameterization for Atmospheric Studies. *NASA. Technol. Memo.* **1999**, *15*, 104606.
57. Chen, F.; Dudhia, J. Coupling an Advanced Land Surface–Hydrology Model with the Penn State–NCAR MM5 Modeling System. Part I: Model Implementation and Sensitivity. *Mon. Weather. Rev* **2001**, *129*, 569–585. [CrossRef]
58. Tewari, M.; Chen, F.; Wang, W.; Dudhia, J.; Lemone, A.; Mitchell, E.; Ek, M.; Gayno, G.; Wegiel, W.; Cuenca, R.H. Implementation and Verification of the Unified Noah Land-Surface Model in the WRF Model. In Proceedings of the 20th Conference on Weather Analysis and Forecasting/16th Conference on Numerical Weather Prediction, Seattle, WA, USA, 14 January 2004.
59. Hong, S.-Y.; Noh, Y.; Dudhia, J. A New Vertical Diffusion Package with an Explicit Treatment of Entrainment Processes. *Mon. Weather. Rev.* **2006**, *134*, 2318–2341. [CrossRef]
60. Lin, Y.-L.; Farley, R.D.; Orville, H.D. Bulk Parameterization of the Snow Field in a Cloud Model. *J. Appl. Meteorol. Climatol.* **1983**, *22*, 1065–1092. [CrossRef]
61. Martilli, A.; Clappier, A.; Rotach, M.W. An Urban Surface Exchange Parameterisation for Mesoscale Models. *Bound. Layer. Meteorol.* **2002**, *104*, 261–304. [CrossRef]
62. Rafee, S.A.A.; Martins, L.D.; Kawashima, A.B.; Almeida, D.S.; Morais, M.V.B.; Souza, R.V.A.; Oliveira, M.B.L.; Souza, R.A.F.; Medeiros, A.S.S.; Guerrero, V.U.; et al. Contributions of Mobile, Stationary and Biogenic Sources to Air Pollution in the Amazon Rainforest: A Numerical Study with the WRF-Chem Model. *Atmos. Chem. Phys.* **2017**, *17*, 7977–7995. [CrossRef]
63. Medeiros, A.S.S.; Calderaro, G.; Guimarães, P.C.; Magalhaes, M.R.; Morais, M.V.B.; Rafee, S.A.A.; Ribeiro, I.O.; Andreoli, R.V.; Martins, J.A.; Martins, L.D.; et al. Power Plant Fuel Switching and Air Quality in a Tropical, Forested Environment. *Atmos. Chem. Phys.* **2017**, *17*, 8987–8998. [CrossRef]
64. Pielke, R.A. Mesoscale Meteorological Modeling Pielke. In *International Geophysics Series*; Academic Press: Cambridge, MA, USA, 2002; Volume 78, ISBN 0125547668.
65. Hallak, R.; Pereira Filho, A.J. Metodology for Performance Analysis of Simulations of Convective Systems in the Metropolitan Area of São Paulo with the ARPS Model: Sensitivity to Variations with the Advection and the Data Assimilation Schemes. *Rev. Bras. De Meteorol.* **2011**, *26*, 591–608. [CrossRef]
66. Zonato, A.; Martilli, A.; di Sabatino, S.; Zardi, D.; Giovannini, L. Evaluating the Performance of a Novel WUDAPT Averaging Technique to Define Urban Morphology with Mesoscale Models. *Urban Clim.* **2020**, *31*, 100584. [CrossRef]
67. Lo, J.C.F.; Lau, A.K.H.; Chen, F.; Fung, J.C.H.; Leung, K.K.M. Urban Modification in a Mesoscale Model and the Effects on the Local Circulation in the Pearl River Delta Region. *J. Appl. Meteorol. Climatol.* **2007**, *46*, 457–476. [CrossRef]
68. Stewart, I.D.; Oke, T.R. Local Climate Zones for Urban Temperature Studies. *Bull. Am. Meteorol. Soc.* **2012**, *93*, 1879–1900. [CrossRef]
69. Conrad, O.; Bechtel, B.; Bock, M.; Dietrich, H.; Fischer, E.; Gerlitz, L.; Wehberg, J.; Wichmann, V.; Böhner, J. System for Automated Geoscientific Analyses (SAGA) v. 2.1.4. *Geosci. Model. Dev.* **2015**, *8*, 1991–2007. [CrossRef]
70. Ching, J.; Mills, G.; Bechtel, B.; See, L.; Feddema, J.; Wang, X.; Ren, C.; Brousse, O.; Martilli, A.; Neophytou, M.; et al. WUDAPT: An Urban Weather, Climate, and Environmental Modeling Infrastructure for the Anthropocene. *Bull. Am. Meteorol. Soc.* **2018**, *99*, 1907–1924. [CrossRef]
71. Stewart, I.D.; Oke, T.R.; Krayenhoff, E.S. Evaluation of the "local Climate Zone" Scheme Using Temperature Observations and Model Simulations. *Int. J. Climatol.* **2014**, *34*, 1062–1080. [CrossRef]
72. Congalton, R.G.; Green, K. *Assessing the Accuracy of Remotely Sensed Data: Principles and Practices*; CRC Press: Boca Raton, FL, USA, 2019.
73. Gohil, K.; Jin, M.S. Validation and Improvement of the WRF Building Environment Parametrization (BEP) Urban Scheme. *Climate* **2019**, *7*, 109. [CrossRef]
74. Chen, F.; Kusaka, H.; Bornstein, R.; Ching, J.; Grimmond, C.S.B.; Grossman-Clarke, S.; Loridan, T.; Manning, K.W.; Martilli, A.; Miao, S.; et al. The Integrated WRF/Urban Modelling System: Development, Evaluation, and Applications to Urban Environmental Problems. *Int. J. Clim.* **2011**, *31*, 273–288. [CrossRef]
75. De la Paz, D.; Borge, R.; Martilli, A. Assessment of a High Resolution Annual WRF-BEP/CMAQ Simulation for the Urban Area of Madrid (Spain). *Atmos. Environ.* **2016**, *144*, 282–296. [CrossRef]

76. *Jornal Oficial Nº 2781*; Londrina Lei Nº 12.236 Dispõe Sobre o Uso e a Ocupação Do Solo No Município de Londrina e Dá Outras Providências. Jornal Oficial do Município de Londrina: Londrina, Brazil, 2015; pp. 1–71.
77. Bechtel, B.; Alexander, P.J.; Beck, C.; Böhner, J.; Brousse, O.; Ching, J.; Demuzere, M.; Fonte, C.; Gál, T.; Hidalgo, J.; et al. Generating WUDAPT Level 0 Data–Current Status of Production and Evaluation. *Urban Clim.* **2019**, *27*, 24–45. [CrossRef]
78. Salfate, I.; Marin, J.C.; Cuevas, O.; Montecinos, S. Improving Wind Speed Forecasts from the Weather Research and Forecasting Model at a Wind Farm in the Semiarid Coquimbo Region in Central Chile. *Wind. Energy* **2020**, *23*, 1939–1954. [CrossRef]
79. Jiménez, P.A.; Dudhia, J.; González-Rouco, J.F.; Montávez, J.P.; García-Bustamante, E.; Navarro, J.; Vilà-Guerau de Arellano, J.; Muñoz-Roldán, A. An Evaluation of WRF's Ability to Reproduce the Surface Wind over Complex Terrain Based on Typical Circulation Patterns. *J. Geophys. Res. Atmos.* **2013**, *118*, 7651–7669. [CrossRef]
80. Jandaghian, Z.; Berardi, U. Comparing Urban Canopy Models for Microclimate Simulations in Weather Research and Forecasting Models. *Sustain. Cities Soc.* **2020**, *55*, 102025. [CrossRef]
81. Brousse, O.; Martilli, A.; Foley, M.; Mills, G.; Bechtel, B. WUDAPT, an Efficient Land Use Producing Data Tool for Mesoscale Models? Integration of Urban LCZ in WRF over Madrid. *Urban Clim.* **2016**, *17*, 116–134. [CrossRef]
82. Ribeiro, I.; Martilli, A.; Falls, M.; Zonato, A.; Villalba, G. Highly Resolved WRF-BEP/BEM Simulations over Barcelona Urban Area with LCZ. *Atmos. Res.* **2021**, *248*, 105220. [CrossRef]
83. De Morais, M.V.B.; de Freitas, E.D.; Guerrero, V.V.U.; Martins, L.D. A Modeling Analysis of Urban Canopy Parameterization Representing the Vegetation Effects in the Megacity of São Paulo. *Urban Clim.* **2016**, *17*, 102–115. [CrossRef]
84. Lemonsu, A.; Masson, V.; Shashua-Bar, L.; Erell, E.; Pearlmutter, D. Inclusion of Vegetation in the Town Energy Balance Model for Modelling Urban Green Areas. *Geosci. Model. Dev.* **2012**, *5*, 1377–1393. [CrossRef]
85. Jacobs, C.; Klok, L.; Bruse, M.; Cortesão, J.; Lenzholzer, S.; Kluck, J. Are Urban Water Bodies Really Cooling? *Urban Clim.* **2020**, *32*, 100607. [CrossRef]
86. Manteghi, G.; bin Limit, H.; Remaz, D. Water Bodies an Urban Microclimate: A Review. *Mod. Appl. Sci.* **2015**, *9*, 1–10. [CrossRef]
87. Theeuwes, N.E.; Solcerová, A.; Steeneveld, G.J. Modeling the Influence of Open Water Surfaces on the Summertime Temperature and Thermal Comfort in the City. *J. Geophys. Res. Atmos.* **2013**, *118*, 8881–8896. [CrossRef]
88. Segal, M.; Leuthold, M.; Arritt, R.W.; Anderson, C.; Shen, J. Small Lake Daytime Breezes: Some Observational and Conceptual Evaluations. *Bull. Am. Meteorol. Soc.* **1997**, *78*, 1135–1147. [CrossRef]
89. Crosman, E.T.; Horel, J.D. Sea and Lake Breezes: A Review of Numerical Studies. *Boundary Layer Meteorol.* **2010**, *137*, 1–29. [CrossRef]
90. Ji, P.; Zhu, C.Y.; Sheng, Y.Y. Effects of urban wetlands with different shapes on the temperature and humidity of ambient environment. *Chin. J. Appl. Ecol.* **2017**, *28*, 3385–3392. [CrossRef]
91. Targino, A.C.; Coraiola, G.C.; Krecl, P. Green or Blue Spaces? Assessment of the Effectiveness and Costs to Mitigate the Urban Heat Island in a Latin American City. *Theor. Appl. Climatol.* **2019**, *136*, 971–984. [CrossRef]
92. Alves Junior, A.P.; Pereira Neto, O.C. O Mapeamento Da Área de Risco à Jusante Do Lago Igapó Em Londrina–PR-Brasil, No Caso de Rompimento Hipotético Da Barragem. *Territorium* **2020**, *27*, 29–40. [CrossRef]
93. Bortolo, C.; Fresca, T. O Lago Igapó: Alguns Elementos Acerca Da Produção Do Espaço Urbano Da Cidade de Londrina-PR. *Revista. ACTA. Geográfica* **2010**, *4*, 161–176. [CrossRef]
94. Larocca, A.G.; Cardoso, C.; Angelis, B.L.D. de O Impacto Da Ocupação de Fundo de Vales Em Áreas Urbanas–Estudo de Caso Lago Igapó Londrina–PR. *Rev. Nac. Gerenciamento Cid.* **2017**, *5*, 1539. [CrossRef]
95. Lopes, J.; Zequi, J.A.C.; Nunes, V.; de Oliveira, O.; de Neto, O.B.P.; Rodrigues, W. Immature Culicidae (Diptera) Collected from the Igapó Lake Located in the Urban Area of Londrina, Paraná, Brazil. *Braz. Arch. Biol. Technol.* **2002**, *45*, 465–471. [CrossRef]
96. Vacario, E.P.L.; Machado, G. Transbordamentos Das Águas Superficiais Em Londrina: O Caso Do Ribeirão Cambé. In *Os. Desafios. da. Geografia. Física. na. Fronteira. do. Conhecimento*; Instituto De Geociências-Unicamp: Campinas, Brazil, 2017; pp. 512–521.
97. Papangelis, G.; Tombrou, M.; Dandou, A.; Kontos, T. An Urban "Green Planning" Approach Utilizing the Weather Research and Forecasting (WRF) Modeling System. A Case Study of Athens, Greece. *Landsc. Urban Plan* **2012**, *105*, 174–183. [CrossRef]
98. Gkatsopoulos, P. A Methodology for Calculating Cooling from Vegetation Evapotranspiration for Use in Urban Space Microclimate Simulations. *Procedia. Environ. Sci.* **2017**, *38*, 477–484. [CrossRef]
99. Marciotto, E.; de Morais, M.V.B. Energetics of Urban Canopies: A Meteorological Perspective. *J* **2021**, *4*, 645–663. [CrossRef]
100. De Morais, M.V.B.; Guerrero, V.V.U.; de Freitas, E.D.; Marciotto, E.R.; Valdés, H.; Correa, C.; Agredano, R.; Vera-Puerto, I. Sensitivity of Radiative and Thermal Properties of Building Material in the Urban Atmosphere. *Sustainability* **2019**, *11*, 6865. [CrossRef]
101. Zong, L.; Liu, S.; Yang, Y.; Ren, G.; Yu, M.; Zhang, Y.; Li, Y. Synergistic Influence of Local Climate Zones and Wind Speeds on the Urban Heat Island and Heat Waves in the Megacity of Beijing, China. *Front. Earth. Sci.* **2021**, *9*, 673786. [CrossRef]
102. Kabano, P.; Lindley, S.; Harris, A. Evidence of Urban Heat Island Impacts on the Vegetation Growing Season Length in a Tropical City. *Landsc. Urban Plan* **2021**, *206*, 103989. [CrossRef]
103. Cheng, V.; Ng, E.; Chan, C.; Givoni, B. Outdoor Thermal Comfort Study in a Sub-Tropical Climate: A Longitudinal Study Based in Hong Kong. *Int. J. Biometeorol.* **2012**, *56*, 43–56. [CrossRef]
104. Mazhar, N.; Brown, R.D.; Kenny, N.; Lenzholzer, S. Thermal Comfort of Outdoor Spaces in Lahore, Pakistan: Lessons for Bioclimatic Urban Design in the Context of Global Climate Change. *Landsc. Urban Plan* **2015**, *138*, 110–117. [CrossRef]

105. Niu, J.; Liu, J.; Lee, T.; Lin, Z.; Mak, C.; Tse, K.-T.; Tang, B.; Kwok, K.C.S. A New Method to Assess Spatial Variations of Outdoor Thermal Comfort: Onsite Monitoring Results and Implications for Precinct Planning. *Build. Environ.* **2015**, *91*, 263–270. [CrossRef]
106. Yoshida, A.; Hisabayashi, T.; Kashihara, K.; Kinoshita, S.; Hashida, S. Evaluation of Effect of Tree Canopy on Thermal Environment, Thermal Sensation, and Mental State. *Urban Clim.* **2015**, *14*, 240–250. [CrossRef]
107. Sharma, A.; Conry, P.; Fernando, H.J.S.; Hamlet, A.F.; Hellmann, J.J.; Chen, F. Green and Cool Roofs to Mitigate Urban Heat Island Effects in the Chicago Metropolitan Area: Evaluation with a Regional Climate Model. *Environ. Res. Lett.* **2016**, *11*, 064004. [CrossRef]
108. Barwise, Y.; Kumar, P. Designing Vegetation Barriers for Urban Air Pollution Abatement: A Practical Review for Appropriate Plant Species Selection. *NPJ. Clim. Atmos. Sci.* **2020**, *3*, 12. [CrossRef]
109. Buccolieri, R.; Santiago, J.-L.; Rivas, E.; Sanchez, B. Review on Urban Tree Modelling in CFD Simulations: Aerodynamic, Deposition and Thermal Effects. *Urban For. Urban Green* **2018**, *31*, 212–220. [CrossRef]
110. Gałecka-Drozda, A.; Wilkaniec, A.; Szczepańska, M.; Świerk, D. Potential Nature-Based Solutions and Greenwashing to Generate Green Spaces: Developers' Claims versus Reality in New Housing Offers. *Urban For. Urban Green* **2021**, *65*, 127345. [CrossRef]
111. Artmann, M.; Kohler, M.; Meinel, G.; Gan, J.; Ioja, I.-C. How Smart Growth and Green Infrastructure Can Mutually Support Each Other—A Conceptual Framework for Compact and Green Cities. *Ecol. Indic.* **2019**, *96*, 10–22. [CrossRef]
112. Coutts, C.; Hahn, M. Green Infrastructure, Ecosystem Services, and Human Health. *Int. J. Environ. Res. Public. Health* **2015**, *12*, 9768–9798. [CrossRef]
113. Edwards, R.C.; Larson, B.M.H.; Church, A. A "Magic Teleportation Machine": Ethnically Diverse Green Space Users Derive Similar Cultural Ecosystem Benefits from Urban Nature. *Urban For. Urban Green* **2021**, *63*, 127409. [CrossRef]
114. Chang, H.-S.; Lin, Z.-H.; Hsu, Y.-Y. Planning for Green Infrastructure and Mapping Synergies and Trade-Offs: A Case Study in the Yanshuei River Basin, Taiwan. *Urban For. Urban Green* **2021**, *65*, 127325. [CrossRef]
115. Brears, R.C. *Blue. and. Green. Cities*; Palgrave Macmillan UK: London, UK, 2018; ISBN 978-1-137-59257-6.
116. Senanayake, I.P.; Welivitiya, W.D.D.P.; Nadeeka, P.M. Urban Green Spaces Analysis for Development Planning in Colombo, Sri Lanka, Utilizing THEOS Satellite Imagery–A Remote Sensing and GIS Approach. *Urban For. Urban Green* **2013**, *12*, 307–314. [CrossRef]